ACS APPLIED MATERIALS & INTERFACES

Research Article

www.acsami.org

Facile Water-based Spray Pyrolysis of Earth-Abundant Cu_2FeSnS_4 Thin Films as an Efficient Counter Electrode in Dye-Sensitized Solar Cells

Rajiv Ramanujam Prabhakar,[†] Nguyen Huu Loc,[†] Mulmudi Hemant Kumar,[†] Pablo P. Boix,[†] Sun Juan,[‡] Rohit Abraham John,[†] Sudip K. Batabyal,*[,†] and Lydia Helena Wong*[,†,‡]

[†]Energy Research Institute, Nanyang Technological University, Singapore

[‡]School of Materials Science and Engineering, Nanyang Technological University, Singapore

Supporting Information

ABSTRACT: A novel approach to produce earth-abundant Cu_2FeSnS_4 (CFTS) thin film using spray pyrolysis of nontoxic aqueous precursors followed by sulfurization is reported. The CFTS phase formation was confirmed by both Raman spectroscopy and X-ray diffraction techniques. Hall measurements of these films reveal p-type conductivity with good charge carrier density and mobilities appropriate for solar harvesting devices. To the best of our knowledge, this is the first report on the electrical properties of solution-processed Cu_2FeSnS_4 thin films estimated using Hall measurements. Dye-sensitized solar cells (DSSC) fabricated with CFTS thin film as a photocathode in iodine/iodide electrolyte exhibit good power conversion efficiency, 8.03%, indicating that CFTS would be a promising cheaper alternative to replace Pt as a counter electrode in DSSCs.

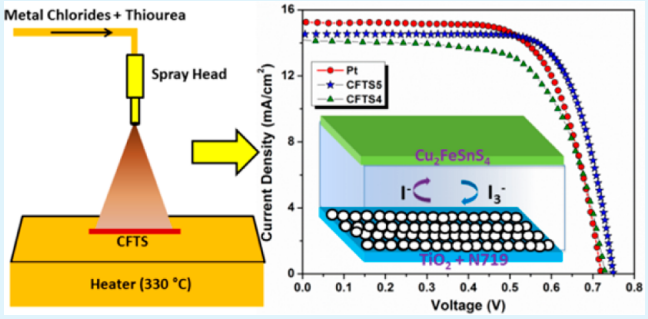

KEYWORDS: *Cu_2FeSnS_4, solution processed thin films, counter electrodes, dye-sensitized solar cells, earth-abundant materials, photovoltaics*

1. INTRODUCTION

Due to its earth abundance and nontoxicity $Cu_2ZnSn(S,Se)_4$ (CZTSSe) is a promising material used in a variety of solar harvesting devices, such as thin film photovoltaics, solar water splitting, and dye-sensitized solar cells (DSSCs).[1−5] Therefore, materials with structures, band gaps, and absorption coefficients analogous to those of CZTSSe, such as Cu_2MSnS_4, where (M = Fe, Co, Ni), have been recently reported for magnetic and photodetector applications.[6,7] Among these, the synthesis of Cu_2FeSnS_4 (CFTS) nanocrystals (NCs) with band gaps of 1.3−1.5 eV have been reported, and their application in photoelectrochemical cells has been explored recently.[8−10] However, these reported methods require solution phase chemical synthesis, which involves the use of toxic organic solvents and post-annealing treatment to remove ligands and improve the electrical conductivity. Therefore, the preparation of CFTS solution by a simple and facile technique (such as spray pyrolysis) using nontoxic precursors would present a significant leap for large-scale commercial applications in photovoltaics.[11−13] Moreover, even though good electrical transport properties of CFTS is essential for its application in solar harvesting devices, the electrical transport characterizations of CFTS nanoparticles or thin film has not been reported to date.

DSSCs have been investigated for the development of low-cost photovoltaics.[14−17] One of the key components in DSSCs is the counter electrode, which collects electrons from the external circuit to reduce I_3^- to I^-.[18] The commonly used counter electrode for the regeneration of iodine/iodide electrolyte is platinum (Pt) due to its high electrocatalytic activity with the iodine/iodide electrolyte system. However, the high cost associated with the scarcity of Pt poses a significant drawback in the large-scale production of DSSCs.[19] Therefore, there is a need for the development of low-cost, earth-abundant, and industrially scalable counter electrodes for DSSCs. Various promising sulfides such as iron sulfide, cobalt sulfide, nickel sulfide, CFTS nanoparticles, and Cu_2ZnSnS_4 (CZTS) have been investigated as a counter electrode in DSSCs.[20−22] Among these, iron sulfide has been shown to demonstrate Pt-like catalytic behavior in DSSC as a counter electrode, but it requires a synthesis technique that involves the use of toxic organic solvents and ligand exchange treatment.[22] Therefore, alternative earth-abundant thin films by a low-cost, nontoxic approach would be essential for the development of Pt-free counter electrodes in DSSCs. As a naturally occurring

Received: June 19, 2014
Accepted: September 26, 2014
Published: September 26, 2014

mineral, CFTS consists of earth-abundant and nontoxic elements, and hence, it is a low-cost replacement of Pt in DSSCs.

In this study, we report a facile method to deposit earth-abundant Cu_2FeSnS_4 (CFTS) thin films by a simple spray pyrolysis followed by sulfurization at different temperatures (400 °C (CFTS4), 500 °C (CFTS5), and 600 °C (CFTS6)). To investigate the crystal structure and the existence of secondary phases after sulfurization at different temperatures, we performed X-ray diffraction and Raman analysis. Hall measurements were performed to investigate the electrical properties such as carrier mobility, type of charge carriers, and carrier density of CFTS. The optical band gaps of CFTS4, CFTS5, and CFTS6 were measured using UV−vis spectroscopy. DSSCs were fabricated with CFTS as the counter electrode, which yielded PCE of 8.03%, in comparison with Pt CE DSSC 7.52%. The catalytic activity of CFTS iodine/iodide electrolyte was investigated using cyclic voltammetry and electrochemical impedance spectroscopy. Finally, our simple thin film fabrication method can be applied to a wide range of magnetic, electronic, and solar harvesting devices.

2. EXPERIMENTAL SECTION

2.1. Synthesis of Cu_2FeSnS_4 Thin Films by Spray Pyrolysis. Cu_2FeSnS_4 thin films were prepared by spray pyrolysis. The precursor solutions used were $CuCl_2{\cdot}2H_2O$ (0.1 M), $FeCl_3{\cdot}6H_2O$ (0.1 M), $SnCl_2{\cdot}2H_2O$ (0.1 M), and thiourea (1 M) with deionized (DI) water as the solvent. The solutions were mixed in a glass bottle with a magnetic stirrer. These precursors were taken in stoichiometric composition of Cu_2FeSnS_4 (thiourea was taken in excess to compensate for the sulfur loss during the spraying) and sprayed onto glass slides on a hot plate at a temperature of 330 °C. After this step, the films were annealed in sulfur ambient in a tube furnace for 30 min. The CFTS thin films were placed at the center of the furnace, where the temperature was maintained at either 400, 500, or 600 °C, and a sulfur powder (25 mg) was placed in a boat at a lower temperature zone of the furnace (200 °C) in Ar atmosphere.

2.2. Morphological, Crystallographic, Electrical, and Optical Properties Investigation of Cu_2FeSnS_4 Thin Films. Scanning electron microscopy (SEM) images were obtained using a field emission scanning electron microscope (FESEM), JEOL JSM-7600F. Crystal structure was investigated using a X-ray diffraction (XRD) by Bruker D8 Advance Diffractometer. Micro Raman spectroscopy was performed using a Renishaw system 2000 (excitation wavelength 514 nm and laser spot size 2 μm). Carrier mobility and carrier density of the CFTS films was measured using an MMR Technologies, Inc. variable temperature Hall measurement system in a four-probe configuration. Four square electrodes (1.6 × 1.6 mm) of aluminum were thermally evaporated in square geometry onto the CFTS films. The absorption spectrum was obtained using a UV−vis spectrophotometer (Shimadzu UV-3600). Thermogravimetric analysis was performed using a TGA Q500 to investigate the growth mechanism of the film after spray pyrolysis.

2.3. Fabrication of Dye-Sensitized Solar Cells with Pt and Cu_2FeSnS_4 as a Counter Electrode and Characterization. The N719 (Dyesol)-sensitized devices were fabricated as reported elsewhere.[23] Details of the DSSC fabrication have been provided in the Supporting Information. Photocurrent density−photovoltage (J−V) characteristics were measured under an illumination of AM 1.5 (100 mW cm^{-2}) using a solar simulator (Sanei Electric, XEC-301S) equipped with a 450 W xenon lamp, which was coupled with an Agilent semiconductor parameter analyzer (4155C). The power of the simulated light was calibrated to 100 mW cm^{-2} by using a silicon reference cell (Fraunhofer) and monitored using a power meter throughout the testing. A black mask (6 × 6 mm) was used in the subsequent photovoltaic studies to avoid the effects of diffusive light on cell performance. Impedance spectroscopy (IS) was measured with an Autolab 302 at different DC bias potentials under the region of interest under dark conditions. The applied voltage perturbation had AC amplitude of 20 mV (rms) with a frequency from 1 MHz to 1 Hz. The spectra were fitted using Z-View software. To investigate the catalytic activities of the prepared counter electrodes, cyclic voltammetry (CV) was performed in a three-electrode system (Pt mesh and SCE as counter and reference electrodes, respectively) with electrolyte described in the DSSC fabrication.

3. RESULTS AND DISCUSSION

The XRD pattern of the as-sprayed films does not show any peaks which indicates that the films are amorphous (Figure S1, Supporting Information). Thermogravimetric (TGA) analysis was performed on the precursor metal chlorides and thiourea to investigate the film growth mechanism after spray pyrolysis (Figure S2, Supporting Information). The precursor metal chlorides and thiourea were mixed and heated from 50 to 400 °C in air, and the weight loss was monitored. The weight loss at 330 °C (temperature of spray pyrolysis) was ∼50%, even though for the formation of CFTS, there should be a weight loss of 70% (by taking into account the molecular weight of (metal chlorides + Thiourea) and the molecular weight of Cu_2FeSnS_4 (section S2, Supporting Information)). This indicates that either the reaction is not fully complete or binary sulfides are formed. Therefore, an additional annealing step in the presence of sulfur vapor (sulfurization) was performed to complete the reaction and improve the crystallinity. The as-sprayed films were brown in color, and the films turned black after sulfurization. The thickness of the films after sulfurization are 400 ± 50 nm, as measured by surface profilometry. Figure 1 shows the X-ray diffraction

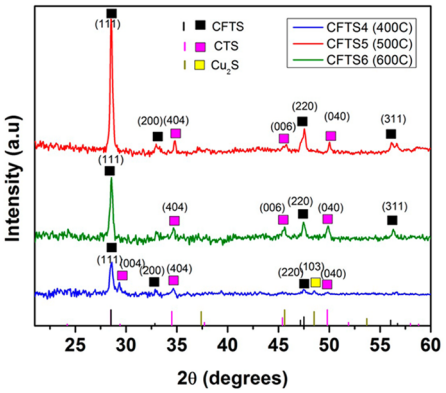

Figure 1. X-ray diffraction pattern of CFTS4, CFTS5, and CFTS6 indicating the presence of CFTS phase.

patterns of CFTS after sulfurization at 400 °C (CFTS4), 500 °C (CFTS5), and 600 °C (CFTS6). The peaks marked with black squares in Figure 1 for CFTS4, CFTS5, and CFTS6 samples can be indexed to Cu_2FeSnS_4, thus confirming the presence of CFTS (JCPDS 70-4373).[9] There were also peaks corresponding to $Cu_2Sn_3S_7$ (CTS) marked by the magenta squares in Figure 1.[24] A peak corresponding to Cu_2S was observed only for CFTS 400 °C. With increasing sulfurization temperature, the intensities of CTS peaks were much lower in comparison to CFTS peaks. However, XRD is not a very conclusive technique to distinguish the various Cu−Sn−S phases because the diffraction peaks overlap for the different phases of Cu−Sn−S.[24] Raman spectroscopy is used to confirm the different phases in the thin films. Figure 2 shows the Raman

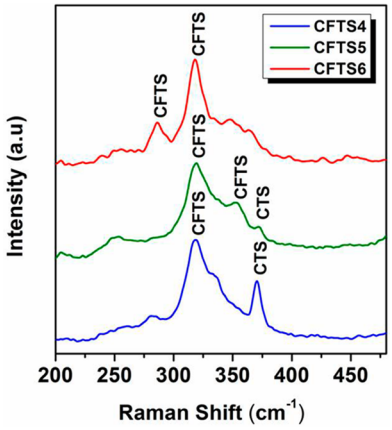

Figure 2. Raman spectra of CFTS4, CFTS5, and CFTS6 showing the presence of CFTS.

spectra of CFTS4, CFTS5, and CFTS6 thin films. For the CFTS4 sample, Raman peaks at 285, 319, and 373 cm^{-1} are observed. The peaks at 285 and 319 can be attributed to Cu_2FeSnS_4[25], and the peak at 373 cm^{-1} is attributed to $Cu_2Sn_3S_7$.[26] For the CFTS5 sample, Raman peaks corresponding to CFTS were observed as labeled in Figure 2. The main feature of these two spectra is the Raman peak at 319 cm^{-1}. This peak (319 cm^{-1}) corresponds to the strongest asymmetry vibration of a pure anion mode of the sulfur atom around the Sn metal, and the peak at 285 cm^{-1} corresponds to a pure anion mode around the Cu cation.[25,27] The CFTS6 sample also exhibited the Raman modes associated with Cu_2FeSnS_4 (labeled in Figure 2). The interesting feature about the Raman spectra of CFTS5 and CFTS6 was that the intensity of the 373 cm^{-1} was very low in comparison to that of CFTS4, possibly indicating that less CTS phase was present in CFTS5 and CFTS6. Therefore, both Raman and XRD data confirm that as the sulfurization temperature increases from 400 to 600 °C, the amount of CFTS increases while the amount of CTS decreases. We speculate that during sulfurization, CTS is formed first followed by the diffusion of Fe inside CTS lattice. As the Fe diffusion is faster at higher temperature, it resulted in a greater amount of CFTS phase.[24] The thickness of the films after sulfurization was found to be 400 ± 50 nm using surface profilometry. The elemental composition was estimated from EDX measurements (Figure S3, Supporting Information) as CFTS4, $Cu_{1.71}Fe_{0.72}Sn_{0.78}S_4$; CFTS5, $Cu_{1.88}Fe_{0.73}Sn_{0.63}S_4$; and CFTS6, $Cu_{1.87}Fe_{0.85}Sn_{1.02}S_4$. All the samples were Cu poor, and CFTS6 was found to be close to the stoichiometric composition. Figure 3A–C shows the SEM images of CFTS4, CFTS5, and CFTS6, respectively (all images obtained at the same magnification). From the SEM images, we can observe an increase in the grain size with an increase in temperature, and it is more obvious in the CFTS6 sample. A

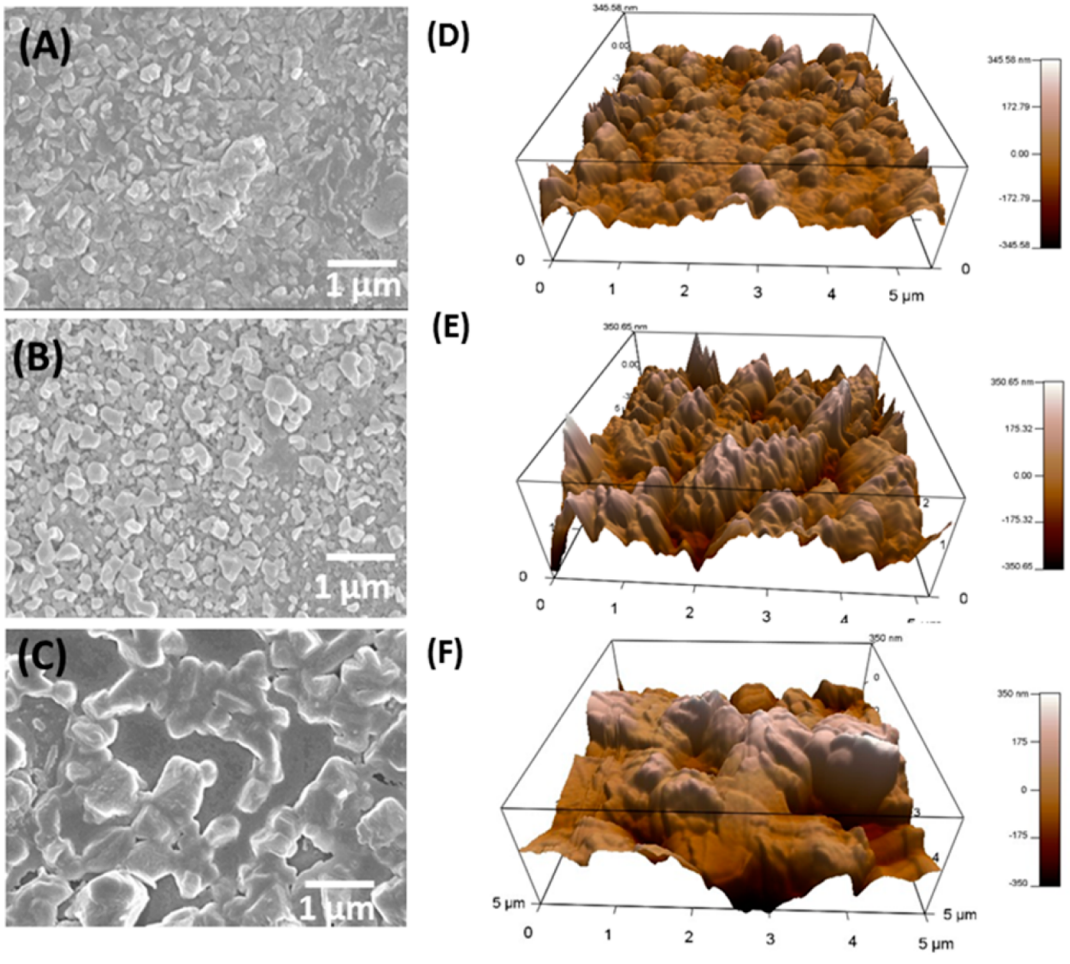

Figure 3. SEM images of (A) CFTS4, (B) CFTS5, and (C) CFTS6 showing the surface morphology. 3-D AFM tapping mode images of (D) CFTS4, (E) CFTS5, and (F) CFTS6 showing the surface morphology.

similar trend was also reported in CZTS with increasing sulfurization temperature.[28] Figure 3D–F shows the 3-D plots of tapping mode AFM images. The surface roughness increases with increasing temperatures (CFTS4, CFTS5, and CFTS6 are ~72, 103, and 123 nm, respectively). The AFM images further elucidate the increasing grain size with increasing sulfurization temperatures.

The electrical properties of the CFTS4, CFTS5, and CFTS6 estimated from Hall measurements are shown in Figure 4. The

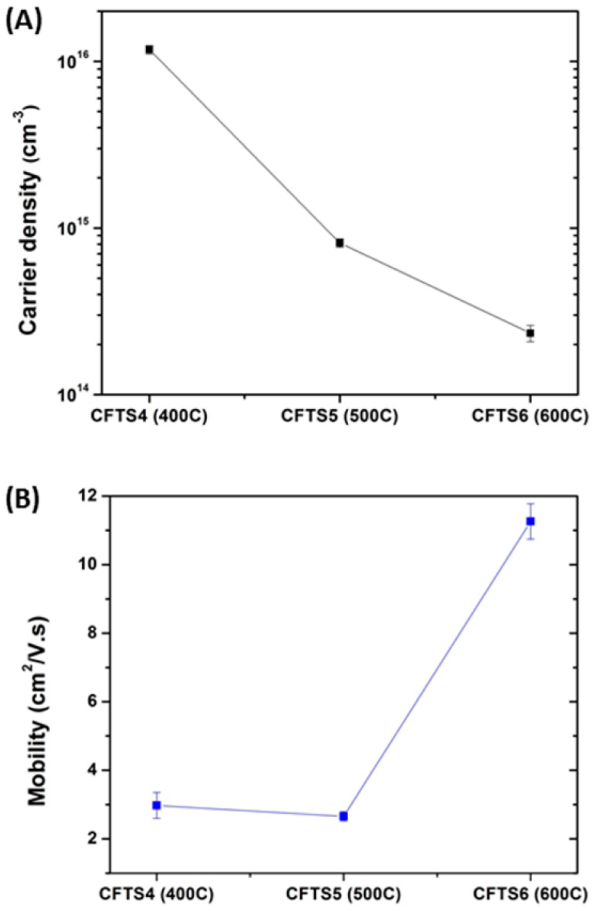

Figure 4. (A) Carrier density and (B) mobility of CFTS4, CFTS5, and CFTS6 obtained from Hall measurements (error bars indicated).

majority carriers in all the films are holes, which indicate p-type conductivity in the films. The carrier mobility in CFTS6 (11.44 cm^2/V·s) films was the highest as compared to CFTS4 (3.04 cm^2/V·s) and CFTS5 (2.51 cm^2/V·s). The carrier mobilites of all CFTS films are comparable with CZTS (6–12 cm^2/V·s), suggesting the potential of CFTS as an absorber layer in thin-film photovoltaics.[29] CFTS5 and CFTS6 exhibit a carrier density of the same order (10^{14}), and CFTS4 exhibits the highest carrier density of the order of 10^{16}. The higher carrier density of CFTS4 in comparison to those of CFTS5 and CFTS6 could be due to the presence of CTS, as some Cu–Sn–S phase was reported to possess metallic electrical characteristics.[30] To the best of our knowledge, our work is the first report on the electrical properties of solution-processed Cu_2FeSnS_4 thin films estimated using Hall measurements. Because CFTS is a possible candidate for solar harvesting devices, the estimation of its band gap is important for practical applications. The band gap was estimated using the equation $(\alpha h\nu)^2 = A(h\nu - E_g)$ and by extrapolating the linear region of the $(\alpha h\nu)^2$ versus $h\nu$ plots and from the intercept on the $h\nu$ axis.[31] Figure 5 shows the $(\alpha h\nu)^2$ versus $h\nu$ plots of CFTS4,

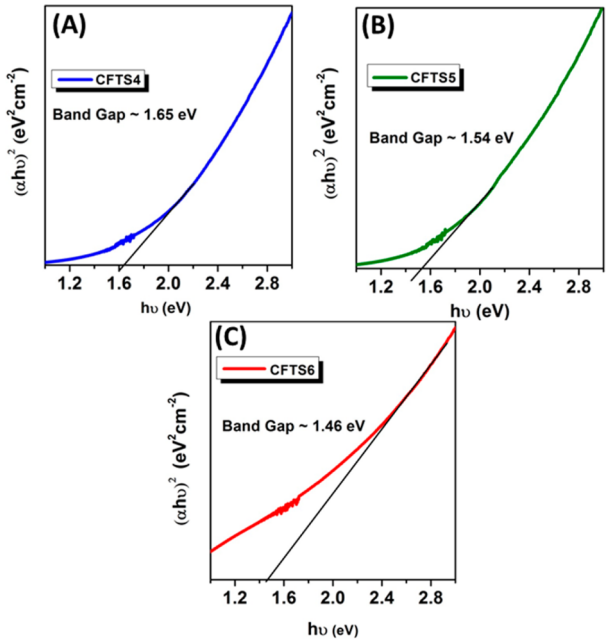

Figure 5. $(\alpha h\nu)^2$ vs $h\nu$ plots of (A) CFTS4, (B) CFTS5, and (C) CFTS6 for band gap estimation.

CFTS5, and CFTS6. The optical band gap values of CFTS4, CFTS5, and CFTS6 are ~1.65, 1.54, and 1.46 eV, respectively, which are similar to the band gaps of CFTS reported in literature.[9] These band gap values suggest that CFTS is a promising material as a light absorber in solar harvesting devices.

DSSCs were fabricated using CFTS thin films as a counter electrode to investigate whether CFTS can be a suitable replacement of Pt in DSSCs. DSSC with CFTS6 as counter electrode was not investigated as the FTO substrates were distorted in the high sulfurization temperatures (Figure S5, Supporting Information). Figure 6 shows the J–V curves of

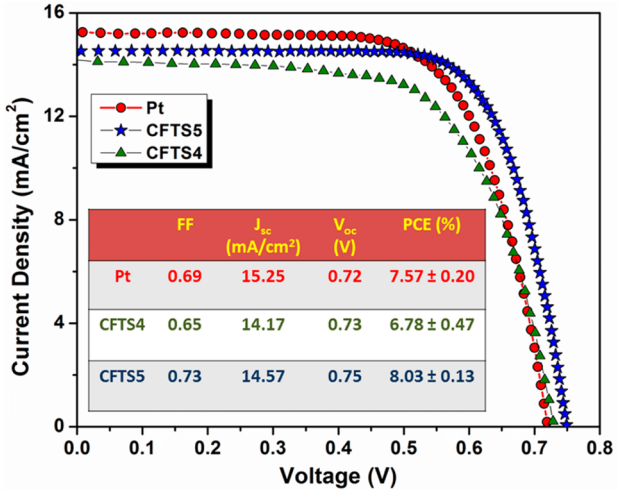

Figure 6. Current density (J)–voltage (V) plots of DSSCs fabricated using Pt and CFTS4 and CFTS5.

dx.doi.org/10.1021/am503888v | ACS Appl. Mater. Interfaces 2014, 6, 17661–17667

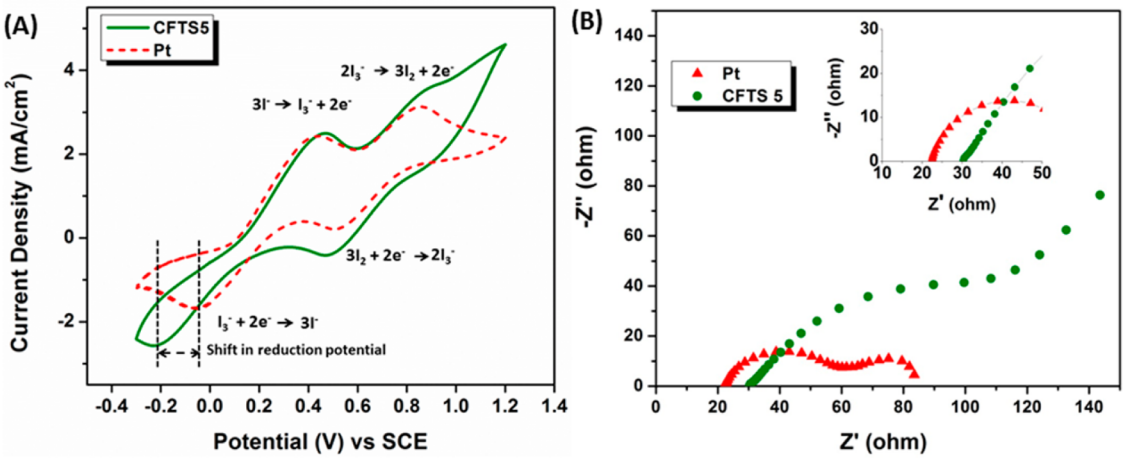

Figure 7. (A) $C-V$ curves of CFTS5 and Pt in iodine/iodide electrolyte. (B) Nyquist plots of symmetric cells (CFTS5 and Pt) measured at a bias of 0.5 V; (inset) magnified plot between 10 and 50 ohm.

DSSCs fabricated using CFTS4, CFTS5, and Pt as counter electrode. It is evident from the DSSC performance (Figure 6 inset) that CFTS5 (8.03%) exhibits a higher power conversion efficiency than a Pt counter electrode (7.57%). The power conversion efficiency of the CFTS4 device (6.78%) was lower than that of Pt counter electrode. This could be due to the presence of the secondary phase like Cu_2S and Cu−Sn−S phases (observed in XRD) which have been shown to have poor catalytic activity in Iodine/Iodide electrolyte.[20,21] The power conversion efficiency exhibited by the CFTS5 device suggests that CFTS can be a viable candidate for the replacement of Pt in DSSCs. It should also be noted that the power conversion efficiency of CFTS5 film (8.03%) as a counter electrode is also much higher in comparison to that of CFTS nanoparticles reported in literature (5.9%).[20] It is possible that the surface stabilizer on the as-synthesized nanoparticles impedes charge transfer, unlike our sprayed CFTS, which does not contain any carbonous impurity. The CFTS5 device was tested after 3 days to investigate its stability. It exhibited a power conversion efficiency of 6.11% (Figure S6, Supporting Information). The current density decreased considerably, and the V_{oc} and fill factor decreased marginally. It is evident from $J-V$ curves that the main improvement in the CFTS5 counter electrode was the fill factor and marginal improvement in V_{oc} (30 mV). Because CFTS5 exhibits very good power conversion efficiency in comparison to Pt-based DSSC, cyclic voltammetry and impedance spectroscopy studies were conducted to understand the reason behind the improved performance of CFTS5 counter electrodes; these studies are discussed in the following sections.

Figure 7A shows the cyclic voltammetry curves of the CFTS5 and Pt performed in a three-electrode system in iodine/iodide electrolyte. The CFTS5 exhibits the typical redox peaks observed when Pt was employed as a working electrode.[32] The cathodic peaks observed in the range of 0.5 V to −0.3 V versus SCE correspond to reduction reactions 1 and 2:[33]

$$I_3^- + 2e^- = 3I^- \quad (1)$$

$$3I_2 + 2e^- = 2I_3^- \quad (2)$$

The $C-V$ curves indicate that the CFTS5 exhibits good catalytic activity in iodine/iodide electrolyte. However, in the $C-V$ curve of CFTS5, it was observed that the reduction peak corresponding to (1) has shifted to negative potentials in comparison to Pt, which may indicate that the CFTS5 can easily reduce the oxidized electrolyte species and regenerates at the counter electrode.[34] This could also result in the marginal improvement of V_{oc} of CFTS5 and such an improvement in V_{oc} has been observed in other sulfide counter electrodes such as $CuInS_2-ZnS$.[34] Therefore, it is concluded that the good catalytic activity of the CFTS5 in iodine/iodide electrolyte is one of the key reasons behind the higher power conversion efficiency.

To understand the electrochemical characteristics of the CFTS counter electrode, electrochemical impedance spectroscopy was performed on symmetric cells. The high-frequency region of the Nyquist plot provides information regarding the R_{ct} (charge transfer resistance) and the double layer capacitance (C_μ).[35] The fitting of the measured spectra to a well-established transmission line model allows the calculation of R_{ct} and C_μ (Figure 7B).[36] The R_{ct} of Pt and CFTS5 are 7.3 and 21.84 Ω·cm^2, respectively. The efficiency of CFTS5 was higher than that of Pt, despite a having a higher R_{ct} than Pt. However, R_{ct} is not the only deciding factor for the counter electrode performance. The double layer capacitance can also provide information on the catalytic activity of the counter electrode. The C_μ for CFTS5 (6.1×10^{-4} F/cm^2) was higher than that of Pt (2.9×10^{-5} F/cm^2), which corresponds to higher surface area and hence higher catalytic activity.[37] Therefore, on the basis of the $C-V$ curves and EIS studies, the improved performance of the CFTS5 DSSC is attributed to the superior catalytic activity of the CFTS5 in iodine/iodide electrolyte.

4. CONCLUSION

In this work, novel earth-abundant Cu_2FeSnS_4 (CFTS) thin films were synthesized using a simple spray pyrolysis technique using aqueous precursor without any organic solvents. Different sulfurization conditions (400, 500, and 600 °C) were used to study the effect of sulfurization temperature on the properties of CFTS thin films. XRD and Raman analysis confirm the presence of CFTS phase. Hall measurements reveal that the CFTS4, CFTS5, and CFTS6 exhibit p-type conductivity and carrier mobilities of ∼2−11 cm^2/V·s. CFTS4, CFTS5, and CFTS6 exhibit band gap in the range of 1.46−1.65 eV. The desirable electrical and optical properties of CFTS thin films indicate that these films can be utilized as an absorber layer in solar energy harvesting devices. DSSCs fabricated with CFTS5,

a counter electrode, exhibit an excellent power conversion efficiency of 8.03%, which is relatively better than that of the Pt counter electrode. On the basis of the $C-V$ curves and EIS studies, the improved performance of the CFTS5 DSSC is attributed to the superior catalytic activity of the CFTS5 in iodine/iodide electrolyte.

■ ASSOCIATED CONTENT

Supporting Information

DSSC fabrication details, XRD of CFTS thin films before sulfurization, TGA analysis of precursors, EDX measurements, raw hall data, SEM of TCOs, and stability of CFTS5 device. This material is available free of charge via the Internet at http://pubs.acs.org.

■ AUTHOR INFORMATION

Corresponding Authors

*E-mail: lydiawong@ntu.edu.sg.
*E-mail: batabyal@gmail.com.

Author Contributions

The manuscript was written through contributions of all authors. All authors have given approval to the final version of the manuscript.

Notes

The authors declare no competing financial interest.

■ ACKNOWLEDGMENTS

This work is supported by Singapore–Berkeley Research Initiative for Sustainable Energy (SinBeRISE) CREATE Programme and NTU-HUJ-BGU Nanomaterials for Energy and Water Management Programme under the Campus for Research Excellence and Technological Enterprise (CREATE) that is supported by the National Research Foundation, Prime Minister's Office, Singapore.

■ REFERENCES

(1) Polizzotti, A.; Repins, I. L.; Noufi, R.; Wei, S.-H.; Mitzi, D. B. The State and Future Prospects of Kesterite Photovoltaics. *Energy Environ. Sci.* **2013**, *6*, 3171–3182.

(2) Woo, K.; Kim, Y.; Yang, W.; Kim, K.; Kim, I.; Oh, Y.; Kim, J. Y.; Moon, J. Band-gap-graded $Cu_2ZnSn(S_{1-x},Se_x)_4$ Solar Cells Fabricated by an Ethanol-based, Particulate Precursor Ink Route. *Sci. Rep.* **2013**, *3*, 3069.

(3) Xie, Y.; Zhang, C.; Yue, F.; Zhang, Y.; Shi, Y.; Ma, T. Morphology Dependence of Performance of Counter Electrodes for Dye-Sensitized Solar Cells of Hydrothermally Prepared Hierarchical Cu_2ZnSnS_4 Nanostructures. *RSC Adv.* **2013**, *3*, 23264–23268.

(4) Wen, X.; Luo, W.; Zou, Z. Photocurrent Improvement in Nanocrystalline Cu_2ZnSnS_4 Photocathodes by Introducing Porous Structures. *J. Mater. Chem. A* **2013**, *1*, 15479–15485.

(5) Saha, S. K.; Guchhait, A.; Pal, A. J. Cu_2ZnSnS_4 (CZTS) Nanoparticle Based Nontoxic and Earth-Abundant Hybrid pn-Junction Solar Cells. *Phys. Chem. Chem. Phys.* **2012**, *14*, 8090–8096.

(6) Cui, Y.; Deng, R.; Wang, G.; Pan, D. A General Strategy for Synthesis of Quaternary Semiconductor Cu_2MSnS_4 (M = Co_2^+, Fe_2^+, Ni_2^+, Mn_2^+) Nanocrystals. *J. Mater. Chem.* **2012**, *22*, 23136–23140.

(7) Murali, B.; Krupanidhi, S. B. Facile Synthesis of Cu_2CoSnS_4 Nanoparticles Exhibiting Red-Edge-Effect: Application in Hybrid Photonic Devices. *J. Appl. Phys.* **2013**, *114*, 144312.

(8) Yan, C.; Huang, C.; Yang, J.; Liu, F.; Liu, J.; Lai, Y.; Li, J.; Liu, Y. Synthesis and Characterizations of Quaternary Cu_2FeSnS_4 Nanocrystals. *Chem. Comm* **2012**, *48*, 2603–2605.

(9) Zhang, X.; Bao, N.; Ramasamy, K.; Wang, Y.-H. A.; Wang, Y.; Lin, B.; Gupta, A. Crystal Phase-Controlled Synthesis of Cu_2FeSnS_4 Nanocrystals with a Band Gap of Around 1.5 eV. *Chem. Commun.* **2012**, *48*, 4956–4958.

(10) Wu, M.; Ma, T. Platinum-Free Catalysts as Counter Electrodes in Dye-Sensitized Solar Cells. *ChemSusChem* **2012**, *5*, 1343–1357.

(11) Prabhakar, R. R.; Pramana, S. S.; Karthik, K. R. G.; Sow, C. H.; Jinesh, K. B. Ultra-Thin Conformal Deposition of $CuInS_2$ on ZnO Nanowires by Chemical Spray Pyrolysis. *J. Mater. Chem.* **2012**, *22*, 13965–13968.

(12) Zeng, X.; Pramana, S. S.; Batabyal, S. K.; Mhaisalkar, S. G.; Chen, X.; Jinesh, K. B. Low Temperature Synthesis of Wurtzite Zinc Sulfide (ZnS) Thin Films by Chemical Spray Pyrolysis. *Phys. Chem. Chem. Phys.* **2013**, *15*, 6763–6768.

(13) Perednis, D.; Gauckler, L. Thin Film Deposition Using Spray Pyrolysis. *J. Electroceram.* **2005**, *14*, 103–111.

(14) Wang, Q.; Ito, S.; Grätzel, M.; Fabregat-Santiago, F.; Mora-Seró, I.; Bisquert, J.; Bessho, T.; Imai, H. Characteristics of High Efficiency Dye-Sensitized Solar Cells. *J. Phys. Chem. B* **2006**, *110*, 25210–25221.

(15) Powar, S.; Daeneke, T.; Ma, M. T.; Fu, D.; Duffy, N. W.; Götz, G.; Weidelener, M.; Mishra, A.; Bäuerle, P.; Spiccia, L.; Bach, U. Highly Efficient p-Type Dye-Sensitized Solar Cells based on Tris(1,2-diaminoethane)cobalt(II)/(III) Electrolytes. *Angew. Chem., Int. Ed.* **2013**, *52*, 602–605.

(16) Listorti, A.; O'Regan, B.; Durrant, J. R. Electron Transfer Dynamics in Dye-Sensitized Solar Cells. *Chem. Mater.* **2011**, *23*, 3381–3399.

(17) Yella, A.; Lee, H.-W.; Tsao, H. N.; Yi, C.; Chandiran, A. K.; Nazeeruddin, M. K.; Diau, E. W.-G.; Yeh, C.-Y.; Zakeeruddin, S. M.; Grätzel, M. Porphyrin-Sensitized Solar Cells with Cobalt (II/III)-based Redox Electrolyte Exceed 12% Efficiency. *Science* **2011**, *334*, 629–634.

(18) Lin, J.-Y.; Tsai, Y.-T.; Tai, S.-Y.; Lin, Y.-T.; Wan, C.-C.; Tung, Y.-L.; Wu, Y.-S. Pulse-Reversal Deposition of Cobalt Sulfide Thin Film as a Counter Electrode for Dye-Sensitized Solar Cells. *J. Electrochem. Soc.* **2013**, *160*, D46–D52.

(19) Wu, M.; Lin, X.; Wang, Y.; Wang, L.; Guo, W.; Qi, D.; Peng, X.; Hagfeldt, A.; Grätzel, M.; Ma, T. Economical Pt-Free Catalysts for Counter Electrodes of Dye-Sensitized Solar Cells. *J. Am. Chem. Soc.* **2012**, *134*, 3419–3428.

(20) Park, J.-Y.; Noh, J. H.; Mandal, T. N.; Im, S. H.; Jun, Y.; Seok, S. I. Quaternary Semiconductor Cu_2FeSnS_4 Nanoparticles as an Alternative to Pt Catalysts. *RSC Adv.* **2013**, *3*, 24918–24921.

(21) Mulmudi, H. K.; Batabyal, S. K.; Rao, M.; Prabhakar, R. R.; Mathews, N.; Lam, Y. M.; Mhaisalkar, S. G. Solution Processed Transition Metal Sulfides: Application as Counter Electrodes in Dye-Sensitized Solar Cells (DSCs). *Phys. Chem. Chem. Phys.* **2011**, *13*, 19307–19309.

(22) Wang, Y.-C.; Wang, D.-Y.; Jiang, Y.-T.; Chen, H.-A.; Chen, C.-C.; Ho, K.-C.; Chou, H.-L.; Chen, C.-W. FeS_2 Nanocrystal Ink as a Catalytic Electrode for Dye-Sensitized Solar Cells. *Angew. Chem., Int. Ed.* **2013**, *52*, 6694–6698.

(23) Ito, S.; Murakami, T. N.; Comte, P.; Liska, P.; Grätzel, C.; Nazeeruddin, M. K.; Grätzel, M. Fabrication of Thin Film Dye-Sensitized Solar Cells with Solar to Electric Power Conversion Efficiency over 10%. *Thin Solid Films* **2008**, *516*, 4613–4619.

(24) Cheng, A.-J.; Manno, M.; Khare, A.; Leighton, C.; Campbell, S. A.; Aydil, E. S. Imaging and Phase Identification of Cu_2ZnSnS_4 Thin Films using Confocal Raman Spectroscopy. *J. Vac. Sci. Technol. A* **2011**, *29*, 051203.

(25) Rincón, C.; Quintero, M.; Moreno, E.; Power, C.; Quintero, E.; Henao, J. A.; Macías, M. A.; Delgado, G. E.; Tovar, R.; Morocoima, M. X-ray Diffraction, Raman Spectrum and Magnetic Susceptibility of the Magnetic Semiconductor Cu_2FeSnS_4. *Solid State. Commun.* **2011**, *151*, 947–951.

(26) Berg, D. M.; Djemour, R.; Gütay, L.; Siebentritt, S.; Dale, P. J.; Fontane, X.; Izquierdo-Roca, V.; Pérez-Rodriguez, A. Raman Analysis of Monoclinic Cu_2SnS_3 Thin Films. *Appl. Phys. Lett.* **2012**, *100*, 192103.

(27) Himmrich, M.; Haeuseler, H. Far Infrared Studies on Stannite and Wurtzstannite Type Compounds. *Spectrochim. Acta, Part A* **1991**, *47*, 933−942.
(28) Junhee, H.; Seung Wook, S.; Myeong Gil, G.; Jin Hyeok, K.; Jeong Yong, L. Crystallization Behaviour of Co-Sputtered Cu_2ZnSnS_4 Precursor Prepared by Sequential Sulfurization Processes. *Nanotechnology* **2013**, *24*, 095706.
(29) Mitzi, D. B.; Gunawan, O.; Todorov, T. K.; Wang, K.; Guha, S. The Path Towards a High-Performance Solution-Processed Kesterite Solar Cell. *Sol. Energy Mater. Sol. Cells* **2011**, *95*, 1421−1436.
(30) Wu, C.; Hu, Z.; Wang, C.; Sheng, H.; Yang, J.; Xie, Y. Hexagonal Cu_2SnS_3 with Metallic Character: Another Category of Conducting Sulfides. *Appl. Phys. Lett.* **2007**, *91*, 143104.
(31) Woo, K.; Kim, Y.; Moon, J. A Non-Toxic, Solution-Processed, Earth Abundant Absorbing Layer for Thin-Film Solar Cells. *Energy Environ. Sci.* **2012**, *5*, 5340−5345.
(32) Huang, Z.; Liu, X.; Li, K.; Li, D.; Luo, Y.; Li, H.; Song, W.; Chen, L.; Meng, Q. Application of Carbon Materials as Counter Electrodes of Dye-Sensitized Solar Cells. *Electrochem. Commun.* **2007**, *9*, 596−598.
(33) Wu, M.; Lin, X.; Hagfeldt, A.; Ma, T. A Novel Catalyst of WO_2 Nanorod for the Counter Electrode of Dye-Sensitized Solar Cells. *Chem. Comm* **2011**, *47*, 4535−4537.
(34) Yi, L.; Liu, Y.; Yang, N.; Tang, Z.; Zhao, H.; Ma, G.; Su, Z.; Wang, D. One Dimensional $CuInS_2$−ZnS Heterostructured Nanomaterials as Low-Cost and High-Performance Counter Electrodes of Dye-Sensitized Solar Cells. *Energy Environ. Sci.* **2013**, *6*, 835−840.
(35) Jiang, Q. W.; Li, G. R.; Liu, S.; Gao, X. P. Surface-Nitrided Nickel with Bifunctional Structure As Low-Cost Counter Electrode for Dye-Sensitized Solar Cells. *J. Phys. Chem. C* **2010**, *114*, 13397−13401.
(36) Fabregat-Santiago, F.; Garcia-Belmonte, G.; Mora-Sero, I.; Bisquert, J. Characterization of Nanostructured Hybrid and Organic Solar Cells by Impedance Spectroscopy. *Phys. Chem. Chem. Phys.* **2011**, *13*, 9083−9118.
(37) Li, G.-R.; Wang, F.; Jiang, Q.-W.; Gao, X.-P.; Shen, P.-W. Carbon Nanotubes with Titanium Nitride as a Low-Cost Counter-Electrode Material for Dye-Sensitized Solar Cells. *Angew. Chem., Int. Ed.* **2010**, *49*, 3653−3656.